

# We are IntechOpen, the world's leading publisher of Open Access books Built by scientists, for scientists

6,900

Open access books available

186,000

International authors and editors

200M

Downloads

Our authors are among the

154

Countries delivered to

TOP 1%

most cited scientists

12.2%

Contributors from top 500 universities



WEB OF SCIENCE™

Selection of our books indexed in the Book Citation Index  
in Web of Science™ Core Collection (BKCI)

Interested in publishing with us?  
Contact [book.department@intechopen.com](mailto:book.department@intechopen.com)

Numbers displayed above are based on latest data collected.  
For more information visit [www.intechopen.com](http://www.intechopen.com)



# Innovative Differential Protection Scheme for Microgrids Based on RC Current Sensor

*Ali Hadi Abdulwahid and Adnan A. Ateeq*

## Abstract

The modern power system and future ones include several intelligent devices. It also integrates renewable energy sources, energy storage, energy microgrid control system, hybrid networks, and smart grids with the wide application of information technology and communication. The most crucial goal in the smart grid application is improving safety reliability within the network. Recent studies have recommended the development of smart grid technology that enhances the reliability of electric power systems increases efficiency and improves the detection of faults for protection; this will reduce the duration of interruption of the number of customers affected by the outages. Moreover, smart grid technology decreases the power loss of energy usage and improves the efficiency of the system. And protection is one of the most important challenges facing smart grid deployment. In this chapter, protection for smart grids using differential relays is presented. The differential scheme is a very reliable method of ensuring the safety of protected areas. This chapter discusses the differential relay parameters with various fault conditions. Therefore, the protection scheme affirms the rapid separation of the fault zone to reduce damage to the equipment. The simulation results show that the method is effective and reliable.

**Keywords:** microgrid, reliability, renewable energy sources, power grids, power distribution, differential protection

## 1. Introduction

The latest revolution in the electricity network technology is called smart grid (SG). Smart grid term describes the future intelligent electric power that using digital technology to monitor and control. In other words, smart grids integrate information and communication intelligently to improve the electricity delivered to customers. It will also enhance safety and reliability, and financial control services in the system. A smart grid is a version of the future power grid that employs advanced equipment and services together with intelligent monitoring, control, communication, and intellectual protection. It is referred to as a revolution in the future of electric power grids because by using applicable technologies, it is a modern and integrated system. With increased energy demands and the expansion of renewable energy sources, power grid systems must be moderated and improved. The smart grid will integrate all types of electric power sources, and accommodate

all means of energy generation and distribution to meet the future demands of energy and its technologies [1].

Quality of power delivery is a significant goal of the smart grid that will provide a variety of needs and options at different costs. Furthermore, smart grids will provide advanced monitoring and control by employing intelligent equipment such as digital sensors, electronic switches, smart energy metering, and creative and advanced communication systems. Its data acquisition and control systems include interactive software, real-time control, and power flow analysis. All different types of renewable energy sources will be interconnected with the energy grid system to improve quality, reliability, and stability by using intelligent and advanced devices. Providing advanced technology such as the smart grid requires a smart and intelligent protection system to improve the efficiency of power delivery to customers, and to reduce outages. Employing the smart grid allows energy consumers to be active participants by providing information and options to control the electric demand balance [2].

The microgrid is used to provide customers with economical and reliable power resources and to make effective use of them through the formation of a smart grid structure during the disturbance. However, the protection of microgrid is a challenging task [3–5]. This chapter discusses the application of differential protection schemes. Issues related to protection include bidirectional power flow; it also handles the decrease in fault current levels [6–8]. The power system must operate safely at all times. The main requirements for power system protection include speed, selectivity, sensitivity, safety, reliability and dependability. The reliability requirements of the protection system ensure that appropriate and operable protective measures taken even when certain parts of the protective device may fail [9].

## 2. Challenges in implementation of smart grids

As shown in **Figure 1**, the key features of the smart grid offer many advantages and prospects in the power industry, thereby revitalizing the socioeconomic strategies of this sector. However, the extensive applications of emerging technologies, if not considered, have vulnerabilities that may result in disasters such as long-term blackouts, economic failure, and so on. **Table 1** provides a brief survey of some of the challenges of smart grid technology [10].

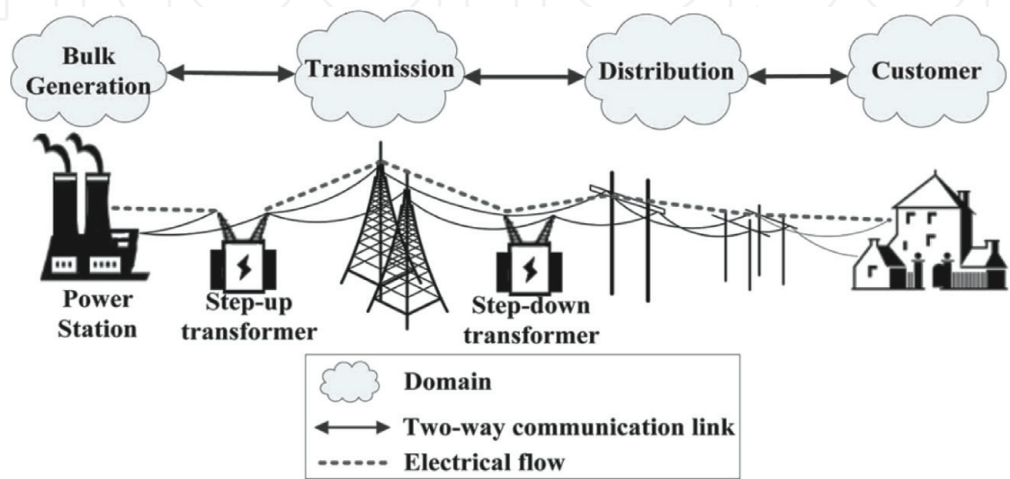


**Figure 1.**  
*Future smart grid processing technology.*

Technology	Challenges	Issues
Self-healing action	Security	Exposed to Internet attacks (spams, worms, virus, and others), question of national security
	Reliability	Failure during natural calamities, system outages, and total blackout
Renewable energy integration	Wind/PV generation and forecasting	Long-term and unpredictable intermittent sources of energy, unscheduled power flow and dispatch
	Power flow optimization	Transmission line congestion and huge investments
	Power system stability	Decoupling causes system stability issues and causes reduced inertia due to high level of wind penetration
Energy systems storage	Complexity	Complex customary design module and networks
	Non-flexibility	Unique designs for all individual networks; no ease of adaptation
Consumer motivation	Security	Malware, data interception, data corruption, illegal power handling, and smuggling
	Privacy	Sharing of data causes privacy invasion, identity spoofing, eavesdropping, and other problems
Reliability	Grid automation	Need for strong data-routing system with secure and private network for reliable protection, control, and communication
	Grid Reconfiguration	Generation demand equilibrium and power system stability with grid complexity
Power quality	Disturbance identification	System instability during sags, dips, or voltage variation such as over-voltages, under-voltages, voltage flickers, and other problems

**Table 1.**  
*Challenges of smart grid technology.*

Extensive research on this technology, which aims to overcome many challenges, has been launched by various universities. The system parameters and configuration of the power grids were investigated more intelligently.

### 3. Rogowski coil current sensor

The Rogowski coil (RC) current sensor works in the same way as a conventional AC core current transformer. They are not closed loops, making the coils open and flexible, and can be wrapped around the conductors [11–13]. RCs can immediately respond to the changing currents, down to a few nanoseconds, due to their low inductance. RC has no iron core to saturate, making it highly linear even when exposed to large currents. Linearity also allows high-current RCs to be determined using smaller reference currents. No danger is observed in opening the secondary winding [14]. Power construction costs and temperature compensation are simple [15–17]. Besides, RC does not use the magnetic core to support two windings. RC is designed with two coils that are electrically connected in the opposite direction, eliminating the electromagnetic field from the outer ring routing. For obtain the current sensor quality, the RC design must meet two important criteria; the first criterion, the mutual inductance  $M$  must have a constant value for any of the main conductor locations inside the coil loop, which can be achieved if the coil core has a constant cross section  $S$ , is perpendicular to the median line and is constructed with



a constant turn density  $n$ . Second, the effects of adjacent conductors carrying a large current to the coil of the output signal should be minimal. The following formula defines mutual inductance  $M$ :

$$M = \mu_o \cdot n \cdot S \tag{1}$$

When the core has a constant cross-section  $S$ ,  $\mu_o$  is the permeability of the free space, and the winding line is perpendicular to the midline  $m$ , with a constant density  $n$ . The output voltage is proportional to the measured rate of change of current, as shown in Eq. (2) [18]:

$$v(t) = -\mu_o n S \frac{di(t)}{dt} = -M \frac{di(t)}{dt} \tag{2}$$

Where  $M$  is the mutual inductance of the coil, also called the sensitivity of the RC. The CT iron core has a nonlinear characteristic and is therefore saturated when a high current or a direct current component is present in primary current. When CT is saturated (that is, the CT ratio error increases), which adversely affects the performance of the relay. **Figure 2** displays the equivalent circuit of a current transformer. The current phase angle between the primary coil and the secondary voltage is almost  $90^\circ$  (due to the coil inductance  $L_s$ ). **Figure 3** shows the equivalent circuit of RCs.

Rogowski coils are linear and can be used in measurement applications. The oscillatory response of RC can be represented by voltage response and natural frequency, as described below:

$$V_o(t) = -M \frac{di(t)}{dt} = -M \frac{di(t)}{dt} \cdot e^{-\xi \omega_n t} \sin \left( \omega_n \sqrt{1 - \xi^2} \right) t, \tag{3}$$

where  $\omega_n$  is the natural frequency, and  $\varepsilon$  is the damping coefficient. As a result, RCs can replace conventional CTs for measurement and protection. IEEE Std C37.235TM-2007 [19] provides guidance on the application of RC sensors when used for protection purposes, review the essential characteristics.

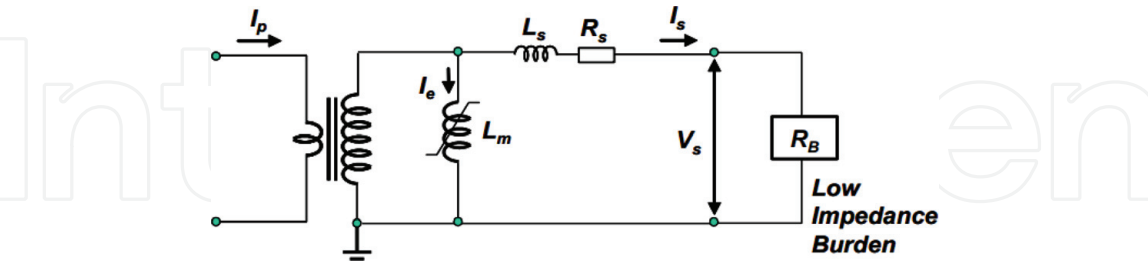


**Figure 2.**  
Current transformer equivalent circuit.

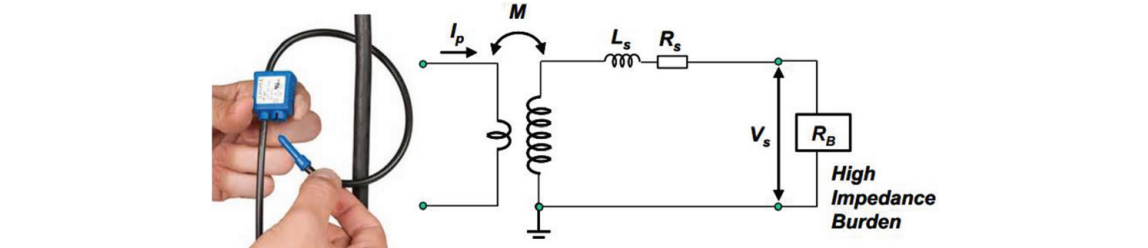


**Figure 3.**  
Rogowski coil equivalent circuits.



In case of no fault, current input protection unit  $I_p$  is to be at all times the same to the current going out of the protected zone. Considering current in transformer A, the pilot wire was carrying current as follows:

$$I_{AS} = a_A I_p - I_{Ae} I_{AS} = a_A I_p - I_{Ae} \quad (4)$$

where  $a_A$  is the conversion ratio for RC A and  $I_{Ae}$  is the secondary excitation current for RC A. Similarly, for current in transformer B, the equation is as follows:

$$I_{BS} = a_B I_p - I_{Be} \quad (5)$$

where  $a_B$  is the conversion ratio for RC B and  $I_{Be}$  is the secondary excitation current for RC B. Considering the equal ratio,  $a_A = a_B = a$ , relay working current  $I_{op}$  is:

$$I_{op} = I_{Ae} - I_{Be} \quad (6)$$

When there was a normal operation or the external fault of the system, the relay's working current  $I_{op}$  was very small, but never tends to zero. Nevertheless, within the time the internal fault was in the protected area, the current was no longer equal to the outgoing current. The operating current of the differential relay is nothing more than an increase of the input current as the same as the feed fault.

$$I_{op} = a(I_{f1} + I_{f2})I_{Ae} - I_{Be} \quad (7)$$

The uniform distribution of the line is as shown in **Figure 5**. Where,  $c_o$  is a shunt capacitance (F/km),  $g_o$  the shunt leakage conductance (S/km),  $l_o$  the series inductance (H/km) and  $r_o$  is a series resistance ( $\Omega$ /km). The distribution of current and voltage along the transmission line is given by the equations of the current and voltage display in the diagram at the ends of the line.

$$-\frac{\partial u}{\partial x} = r_o i + l_o \frac{\partial i}{\partial t} \quad (8)$$

$$-\frac{\partial i}{\partial x} = g_o u + c_o \frac{\partial u}{\partial t} \quad (9)$$

By reducing Eqs. (5) and (6) to their frequency domain,

$$\begin{bmatrix} U_m \\ I_m \end{bmatrix} = \begin{bmatrix} \text{ch}(\gamma l_{nm}) & -Z_c \text{sh}(\gamma l_{nm}) \\ \text{sh}(\gamma l_{nm})/Z_c & -\text{ch}(\gamma l_{nm}) \end{bmatrix} \begin{bmatrix} U_n \\ I_n \end{bmatrix} \quad (10)$$

where  $\text{sh}(\gamma l_{nm})$  and  $\text{ch}(\gamma l_{nm})$  = hyperbolic function,  $Z_c$  = characteristic impedance,  $\gamma$  = the propagation constant and both are frequency dependent;  $l_{nm}$  = distance from end to end m.

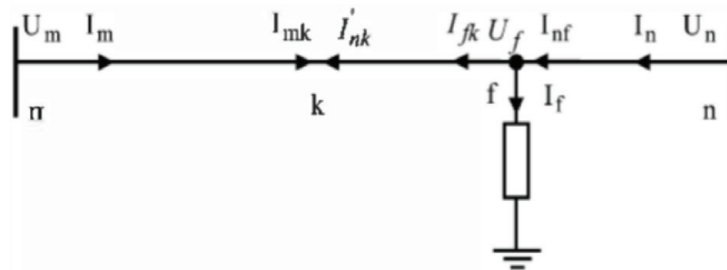


**Figure 5.**  
Transmission line model with a fault located inside the two ends.

By considering the appropriate characteristic impedance and propagation constant, we can apply the above conversion method to the zero, positive and negative sequence components of the current. In this paper, the “0,” “1,” and “2” subscripts were described as zero, positive, and negative sequences, respectively.

$$I_{mk0} = I_{m0} \text{ch}(\gamma_0 l_{mk}) - \frac{U_{m0}}{Z_{c0}} \text{sh}(\gamma_0 l_{mk}) \quad (11)$$

$$I_{mk1} = I_{m1} \text{ch}(\gamma_1 l_{mk}) - \frac{U_{m1}}{Z_{c1}} \text{sh}(\gamma_1 l_{mk}) \quad (12)$$

$$I_{mk2} = I_{m2} \text{ch}(\gamma_2 l_{mk}) - \frac{U_{m2}}{Z_{c2}} \text{sh}(\gamma_2 l_{mk}) \quad (13)$$

$$I_{nk0} = I_{n0} \text{ch}(\gamma_0 l_{nk}) - \frac{U_{n0}}{Z_{c0}} \text{sh}(\gamma_0 l_{nk}) \quad (14)$$

$$I_{nk1} = I_{n1} \text{ch}(\gamma_1 l_{nk}) - \frac{U_{n1}}{Z_{c1}} \text{sh}(\gamma_1 l_{nk}) \quad (15)$$

$$I_{nk2} = I_{n2} \text{ch}(\gamma_2 l_{nk}) - \frac{U_{n2}}{Z_{c2}} \text{sh}(\gamma_2 l_{nk}) \quad (16)$$

where  $l_{mk}$  and  $l_{nk}$  = distance of point k from end m and n respectively.

$$a = e^{j2\pi/3}$$

$$\begin{bmatrix} I_{mka} \\ I_{mkb} \\ I_{mkc} \end{bmatrix} = \begin{bmatrix} 1 & 1 & 1 \\ 1 & a^2 & a \\ 1 & a & a^2 \end{bmatrix} \begin{bmatrix} I_{mk0} \\ I_{mk1} \\ I_{mk2} \end{bmatrix} \quad (17)$$

Similarly, the relationship to current is as below:

$$\begin{bmatrix} I_{nka} \\ I_{nkb} \\ I_{nkc} \end{bmatrix} = \begin{bmatrix} 1 & 1 & 1 \\ 1 & a^2 & a \\ 1 & a & a^2 \end{bmatrix} \begin{bmatrix} I_{nk0} \\ I_{nk1} \\ I_{nk2} \end{bmatrix} \quad (18)$$

If the fault is outside the protected area or there is no fault in the system, then the phase current should satisfy the following equation:

$$I_{mk\varnothing} = -I_{nk\varnothing} \quad (19)$$

where  $\varnothing = a, b, c$  shows the phase from where the current belong to.

The following explanation makes it possible to understand the actual current and the position where the fault and the derivation of the current occur. To calculate the fault location of the current and voltage from the end n,

$$U_{f0} = U_{n0} \text{ch}(\gamma_0 l_{nf}) - I_{n0} Z_{c0} \text{sh}(\gamma_0 l_{nf}) \quad (20)$$

$$U_{f1} = U_{n1} \text{ch}(\gamma_1 l_{nf}) - I_{n1} Z_{c1} \text{sh}(\gamma_1 l_{nf}) \quad (21)$$

$$U_{f2} = U_{n2} \text{ch}(\gamma_2 l_{nf}) - I_{n2} Z_{c2} \text{sh}(\gamma_2 l_{nf}) \quad (22)$$

$$I_{f0} = I_{n0} \text{ch}(\gamma_0 l_{nf}) - \frac{U_{n0}}{Z_{c0}} \text{sh}(\gamma_0 l_{nf}) \quad (23)$$

$$I_{f1} = I_{n1} \text{ch}(\gamma_1 l_{nf}) - \frac{U_{n1}}{Z_{c1}} \text{sh}(\gamma_1 l_{nf}) \quad (24)$$

$$I_{f2} = I_{n2} \text{ch}(\gamma_1 l_{nf}) - \frac{U_{n2}}{Z_{c2}} \text{sh}(\gamma_1 l_{nf}) \quad (25)$$

The differential current is the actual measure of relay operation. In addition, the brake current is one of the avoided currents of the mal-tripping differential relay. The effect of this current has been in breaking the relay.

$$I_B = |I_{mk1} + I_{nk1}| \quad (26)$$

$$I_B = |I_{mk1} + I_{nk} - I_{f1} \text{ch}(\gamma_1 l_{fk})| \quad (27)$$

The effects of the capacitive current can be cancelling with any of the use of the following techniques. Shunt Reactor, Phasor Compensation algorithm, Capacitor Current Compensation, and Bergeron line Model.

In reality, the proposal is a reliable method for the protection system. Since each current transformer and circuit breaker can only declare a line, it is usual to protect by the use of two side current transformers and circuit breakers. The currents on both sides were compared. Under normal conditions or for defects outside the protected area, the current Bas-Bar A is equal to the current Bas-Bar B. Thus, the currents in the secondary current transformer were equal; no current flowed through the relay current. If a fault occurs in the protected zone, the secondary transformer currents of Bas-Bar A and Bas-Bar B will not be the same, and there will be a current flowing through the relay current, as shown **Figure 6**.

The differential protection ratio, by using a multi-slope feature of the relay was inserted into the new relay for its excellent compromise between reliability and sensitivity. The components of the relay compared the different current  $I_{diff}$  (also called operating current), and the restraining current  $I_{bias}$  are expressed in Eqs. (28) and (29) [20–24].

$$I_{diff} = |I'_{As} + I'_{Bs}| \quad (28)$$

$$I_{bias} = (|I'_{As}| + |I'_{Bs}|)/2 \quad (29)$$

where  $I'_{As}$  and  $I'_{Bs}$  are secondary RC phasor currents.

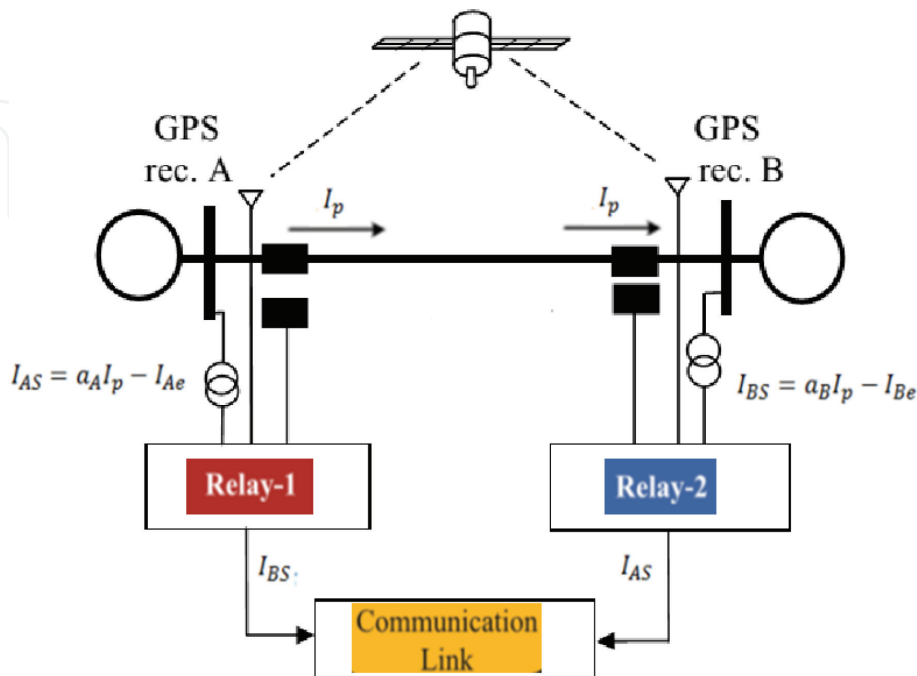


**Figure 6.**  
Differential relay currents at the external fault.



## 5. SCADA systems

It is considered as a means of monitoring and control of power plants also used in renewable power plants and these systems transfer data to the heart of the system which is a master computer and receives orders from many remote terminals; **Figure 7** illustrates the structure of the SCADA system, the SCADA system includes the following:

1. RTUs or PLC which transfers information to the central unit and transfers orders to equipment.
2. Radio system or satellites to secure communication between central units and distributed areas away from the focal point.
3. The software package used in the system.

The operation of electricity distribution networks is monitored and controlled by supervisory control and data acquisition (SCADA) systems. SCADA systems are linked through various communications networks such as microwave and optical fiber networks to ensure the functioning of the system. They are used to connect transmission substations with the major generators to facilitate an integrated system. The operation of the methods of communication in the networks of energy is produced by lines along the system with advanced optical networks. The loss of these communication cables is possible and could make the protection and monitoring of the network more complex. Using advanced wireless communication and sensing devices could improve the control and monitoring of the entire system. Intelligent Electronic Devices (IED) for monitoring and control to improve the technology of smart grids, and. IEDs can be installed and distributed within the system to be used for protection and monitoring [24–28]. These devices are

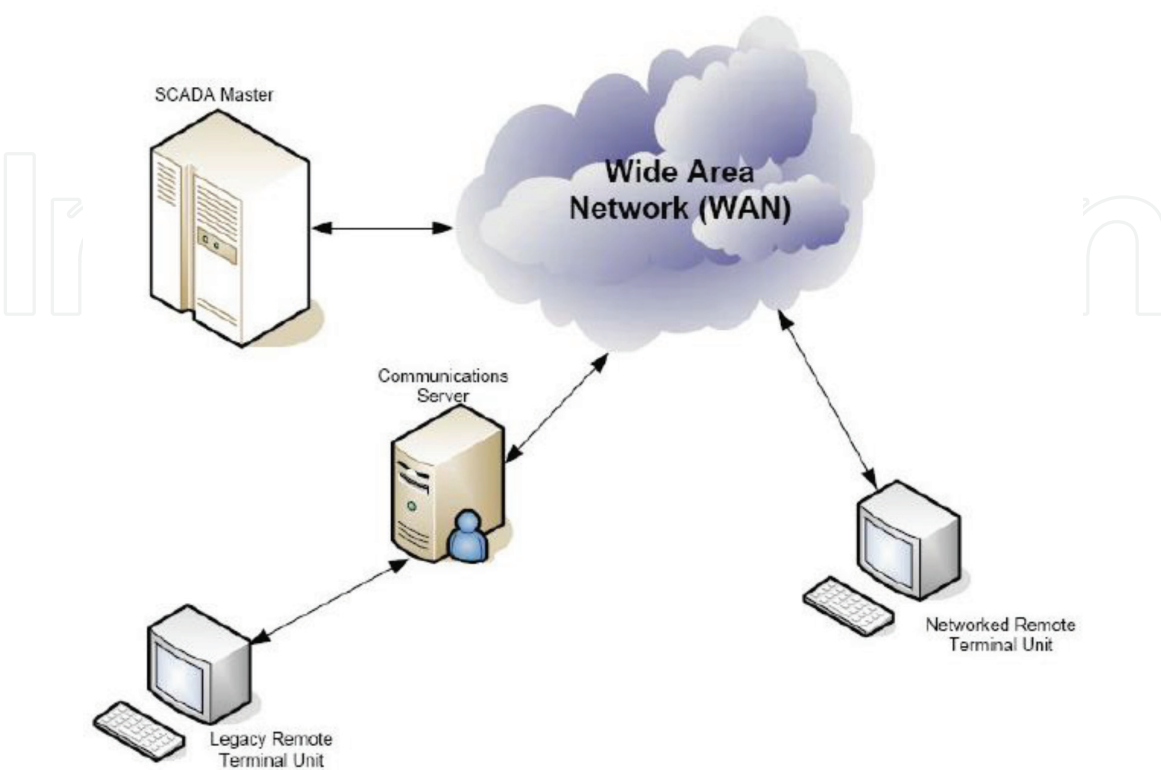


**Figure 7.**  
*Network monitoring and control by supervisory control and data acquisition systems (SCADA).*

interconnected and can be communicated to the central IED, which is implemented in the substation. On the other hand, IEDs can also monitor and update the electric flow of real-time status and can be used to manage and control the network. **Figure 7** shows the monitoring and control by supervisory control and data acquisition system for smart grid technology.

6. System modeling

The simulation of line differential protection is presented in Simulink/MatLab environment, as shown in **Figure 8**.

It simulates three-phase, the system components are a transmission line with PV arrays (800 kW), Wind farm (9 MW), Resistive load (45 kW, 100 kW), 25 kV distribution Bus, and the utility grid. The proposed settings of the protection scheme for transmission lines from Bus-Bar 7 to Bus-Bar 9, and the information corresponding to the lines are listed in **Table 2**, where is the rated secondary current. In this study, is taken to be 1 Amp. According to the value of, the following constants are:

$I_O = 0.3, \quad I_{S2} = 0.2, \quad K_1 = 0.35, \quad K_2 = 1.2;$

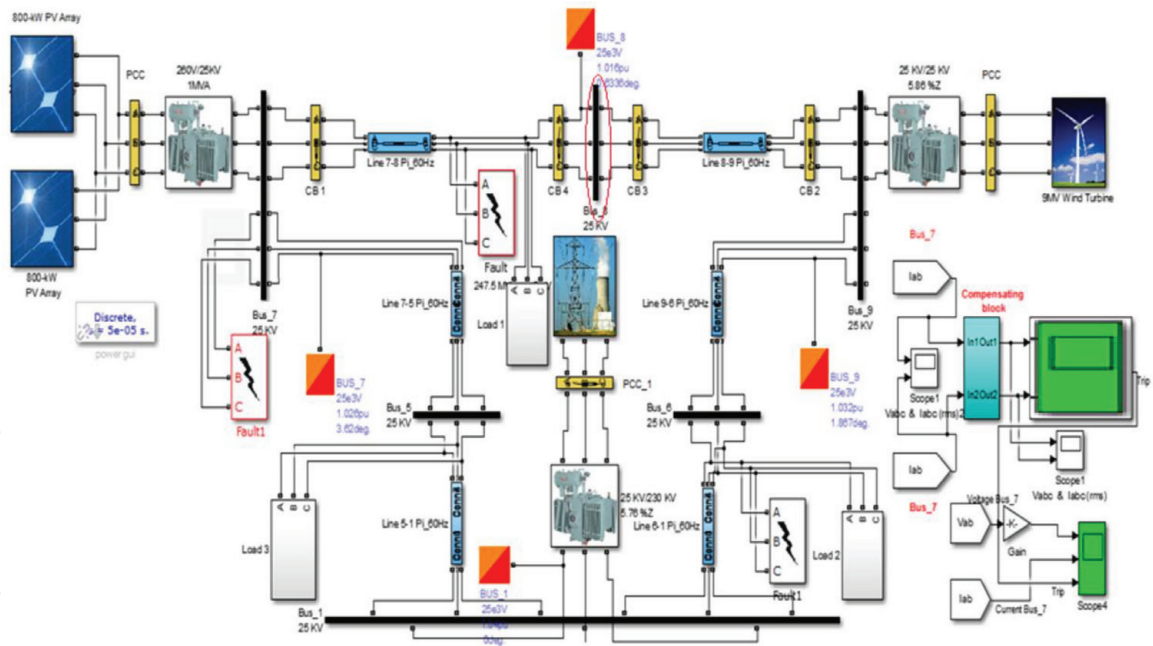


**Figure 8.**  
*Simulation representation of the differential protection scheme.*

Relay setting	Range
Differential current setting	(0.2–2.0 In)
Bias current threshold setting	(1–30)
Lower percentage bias setting	(0.3–1.5)
Higher percentage bias setting	(0.2–2.0 In)

**Table 2.**  
*Relay setting ranges.*

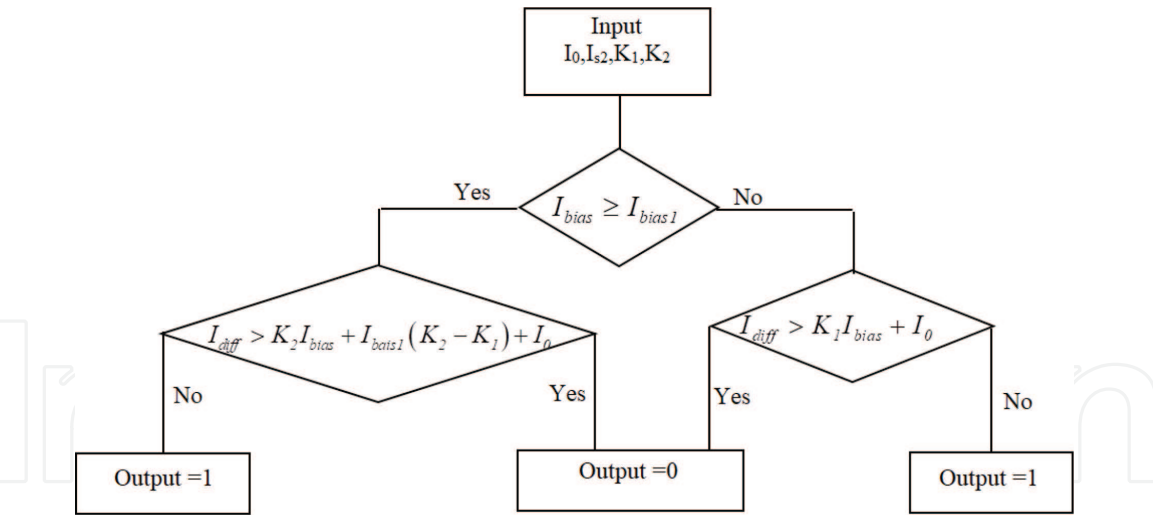


**Figure 9.**  
Flowchart for decision block.

where  $I_n$  is the current rating of the secondary current transformer;  $I_0$  is the differential current at zero bias current;  $I_{bias}$  is the bias current when the relay characteristic starts to change; and  $K_1$ ,  $K_2$  is the percentage biases. These constants can be obtained from the relay characteristic, which is used in relay operations. The differential protection operating region is above the slope of the characteristic, and the restraining of the region is below the slope of the characteristic. The dual slope bias technique is used to improve stability through fault and external fault CT saturation to provide further security. To achieve the appropriate setting, the characteristics of the relay to be applied must be considered. Three adjustable values (from the relay manual) are recommended as follows.

The block consists of a relay that is divided into two units, as shown in **Figure 9**.

## 7. Simulation results and discussion

Differential protection between the two circuit breaker CBs, are known the local side (CB1) and far side (CB2), the Current Sensors RCA and RCB are installed at the Bus-Bar (7 and 9), to measure the current and voltage per phase. The current and voltage of each phase of the analog signal are converted into digital data using an analog-to-digital converter (ADC). The local side is directly connected to the relay, whereas the far side is connected through the delay block. Channel time delay is set at 27 ms, the output of the differential relay block is binary (0, 1). When disturbances happen in the protected zone, a current difference between the two CBs (local and remote) exists. Thus, the relay sends a signal tripping to isolate the defective zone from the rest of the protection scheme. In this study, we propose that the fault will occur in the middle of the transmission line, starting at 0.3 ms. In the fault parameter block, the fault type is simulated separately using MATLAB. This section investigates the cases of faults (internal and external).

Five cases have been tracked: Case 1, single line to ground fault (SLGF); Case 2, line-to-line fault (LLF); Case 3, double line to ground fault (2LGF); Case 4, three-line fault (3LF); and Case 5, three line to ground fault (3LGF). The main principle of the differential relay should be compared for both ends of the protected area. Modeling for each case is similar through comparison of the current at both ends.

All used case results are indicated in **Figures 10–24**. Three diagrams, namely, remote, local, and differential, are presented in every figure. Remote and local measurements are conducted separately; each colour in this diagram represents one



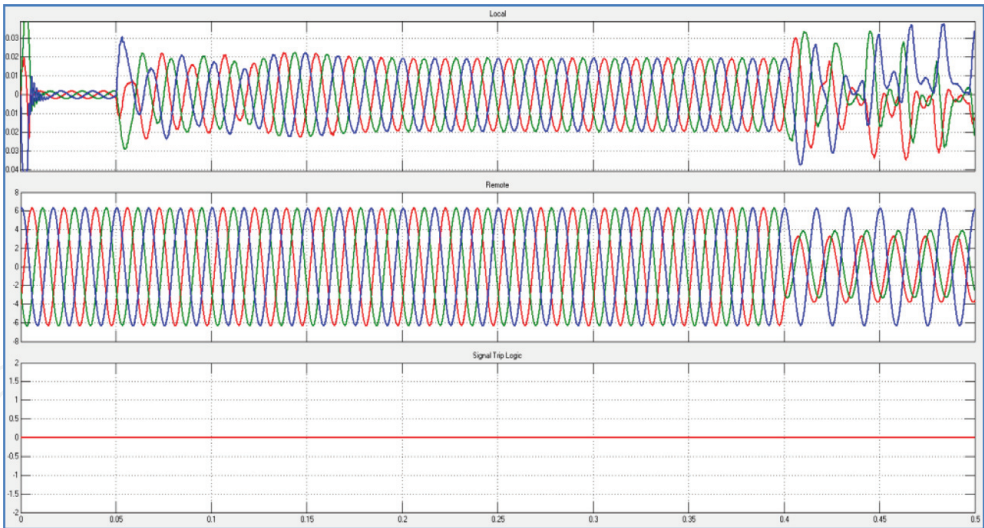


**Figure 10.**  
*SLGF current waveform.*

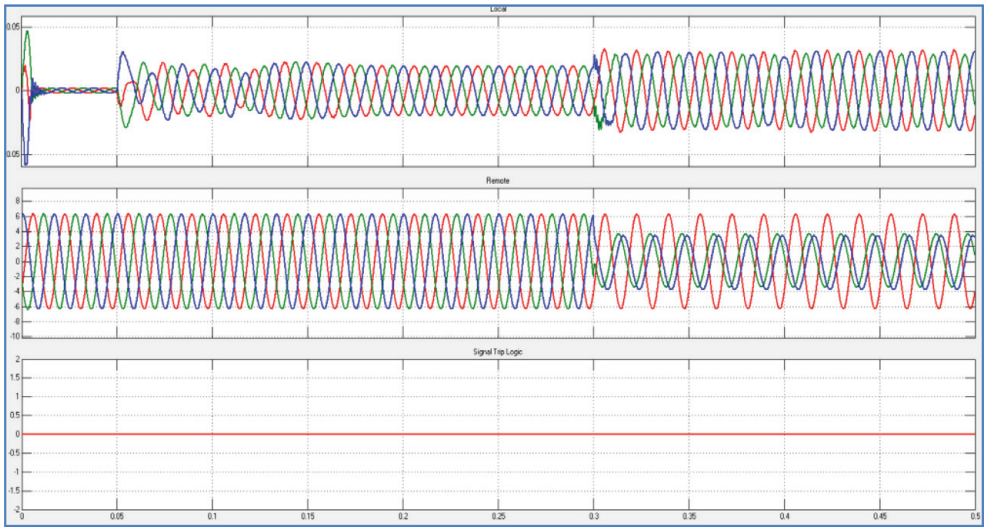


**Figure 11.**  
*SLGF voltage waveform.*

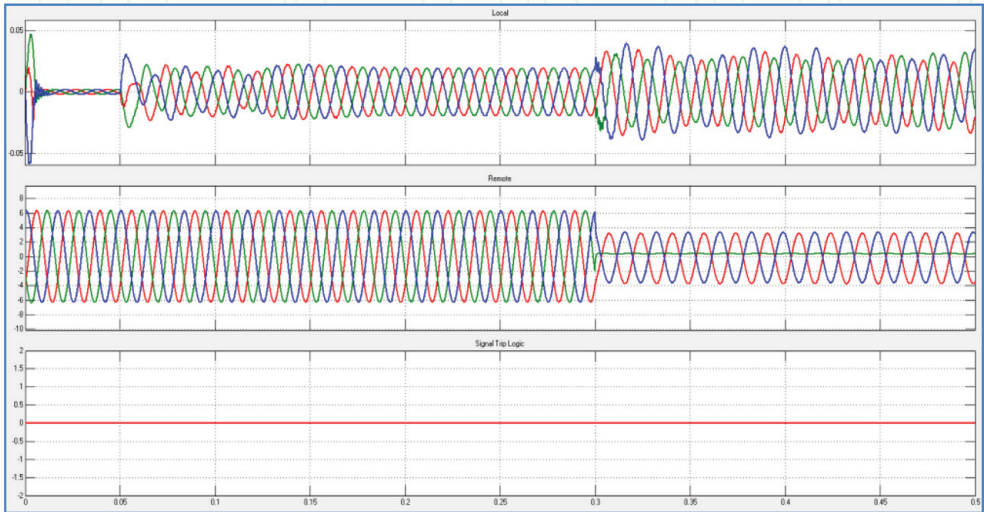


**Figure 12.**  
*2LGF current waveform.*

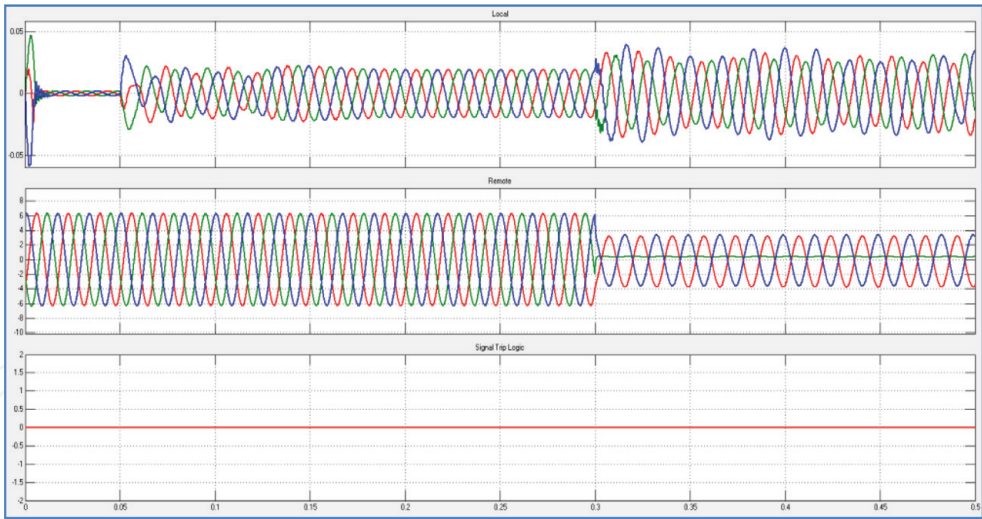


**Figure 13.**  
*2LGF voltage waveform.*

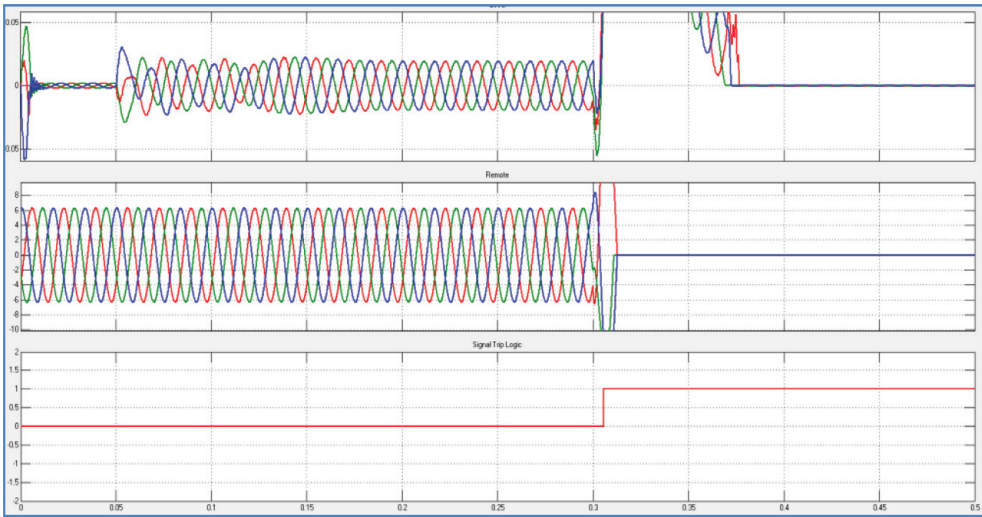


**Figure 14.**  
*SLGF (A) current waveform.*

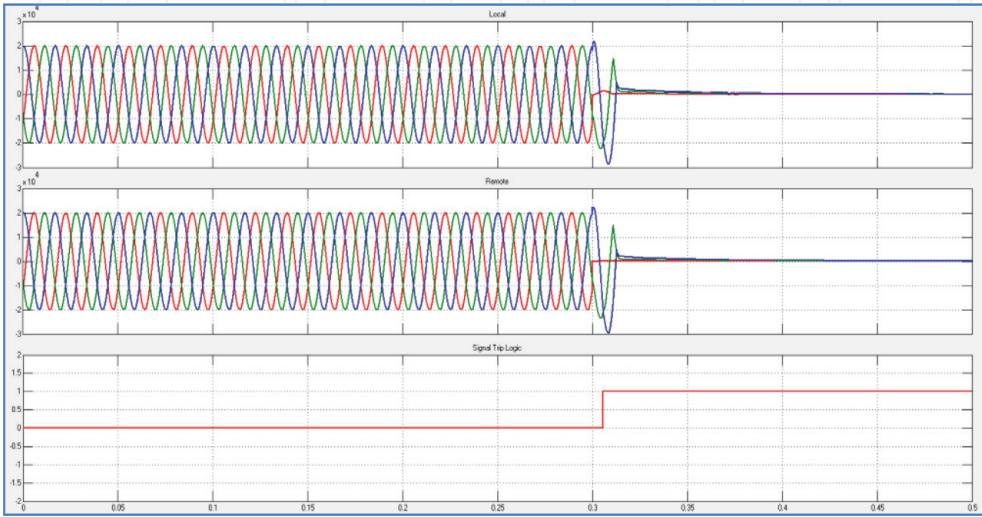


**Figure 15.**  
*SLGF (A) voltage waveform.*



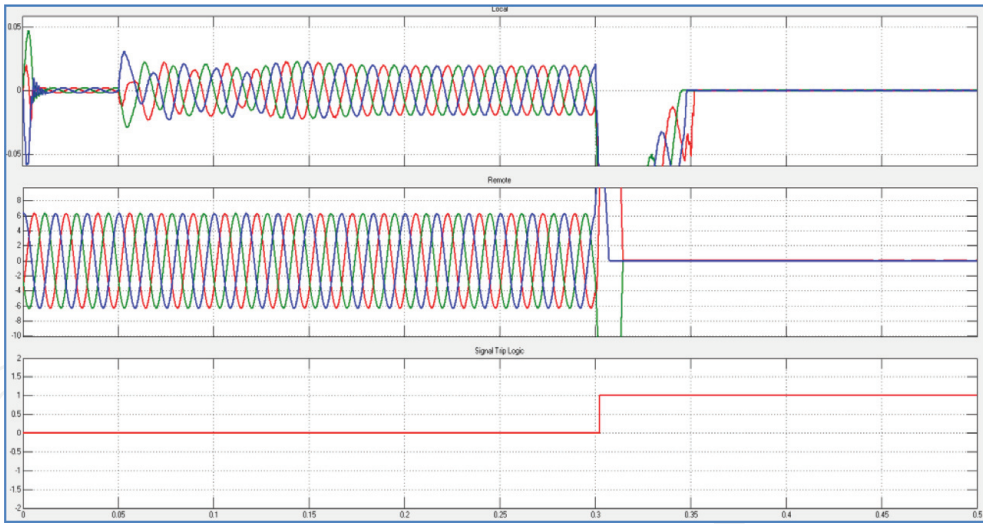


**Figure 16.**  
*Double-line (A and B) fault current waveform.*

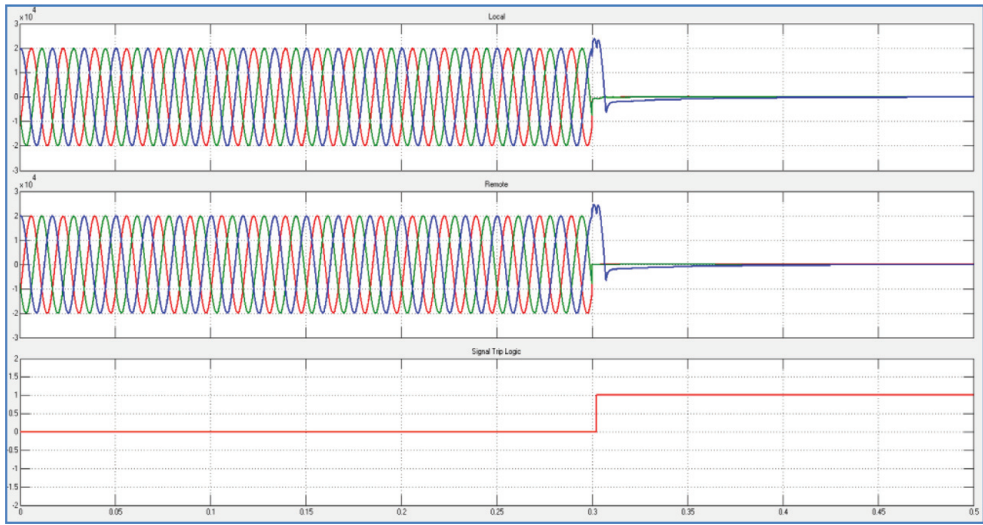


**Figure 17.**  
*Double-line (A and B) fault voltage waveform.*

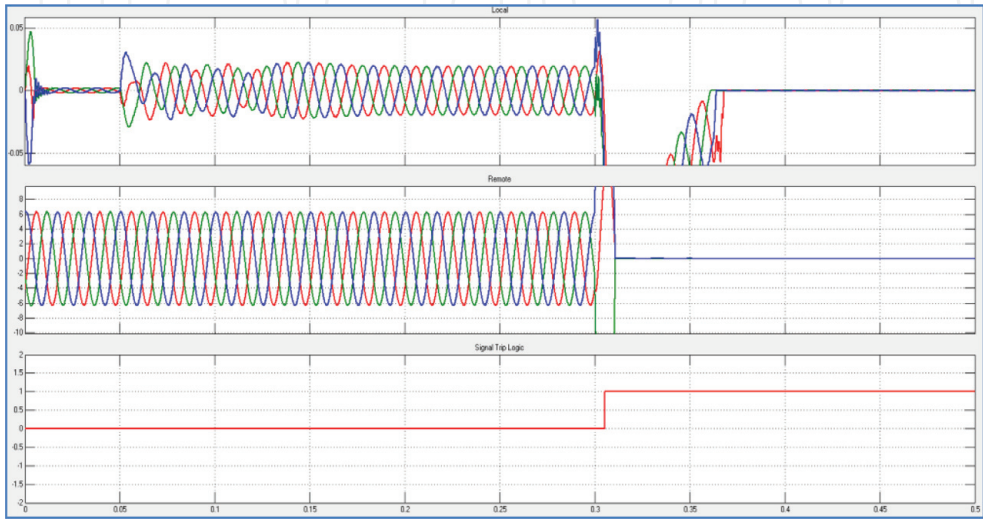


**Figure 18.**  
*2LGF (B and C) current waveform.*

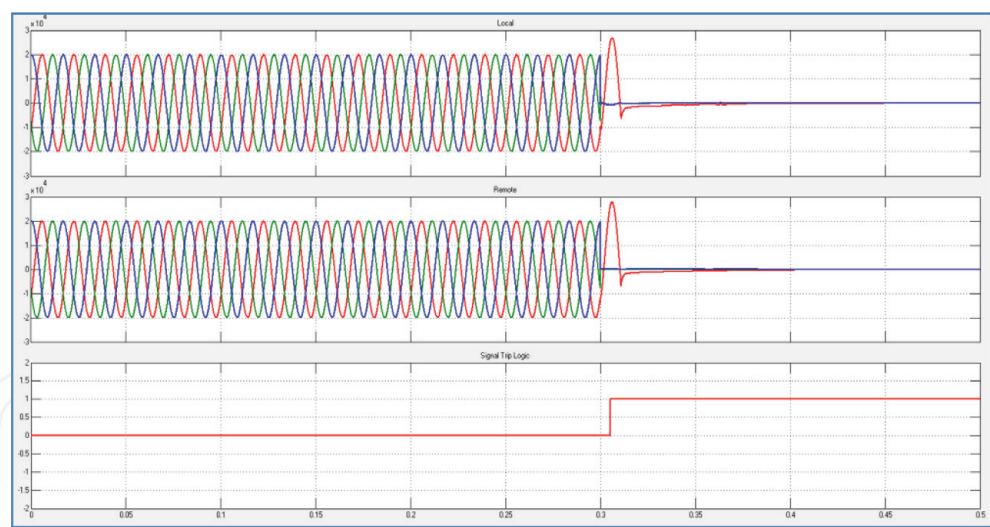


**Figure 19.**  
*2LGF (B and C) voltage waveform.*

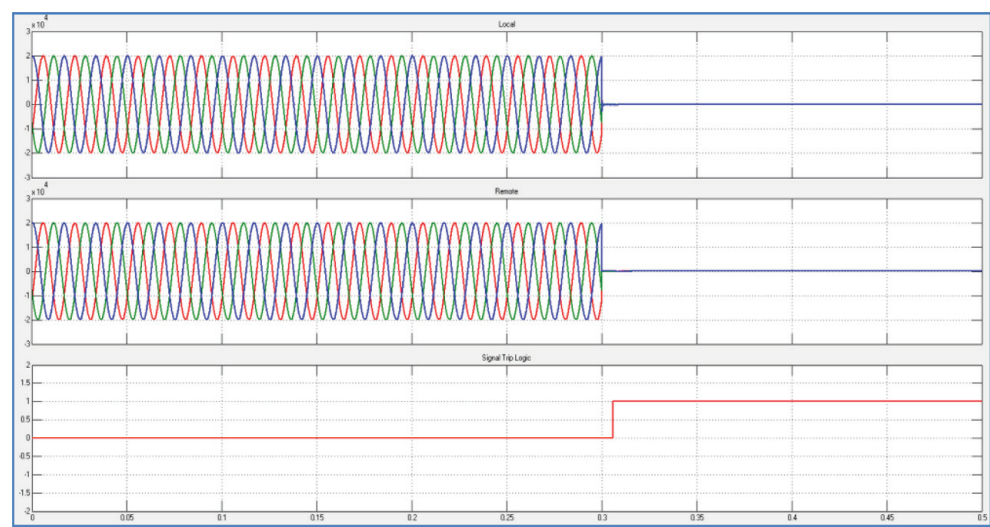


**Figure 20.**  
*3LF current waveform.*

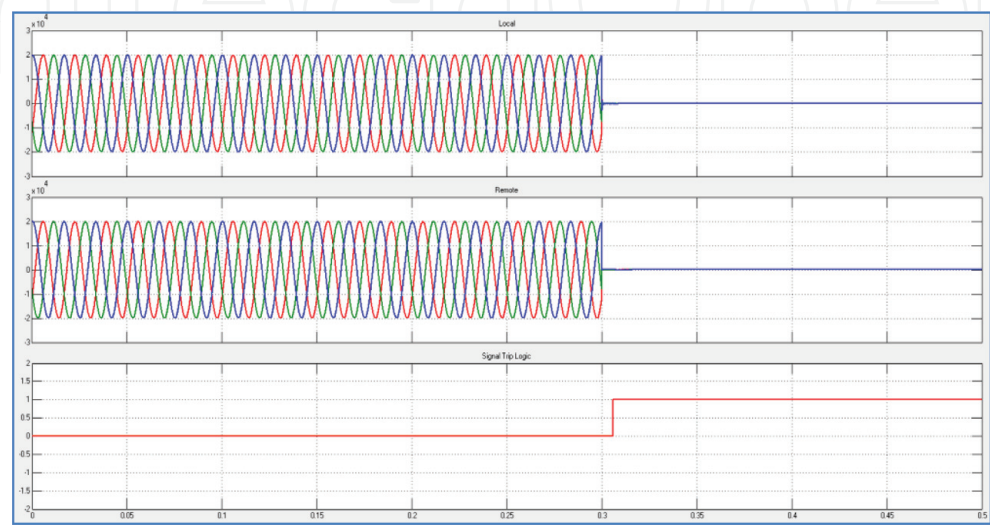


**Figure 21.**  
*3LF voltage waveform.*

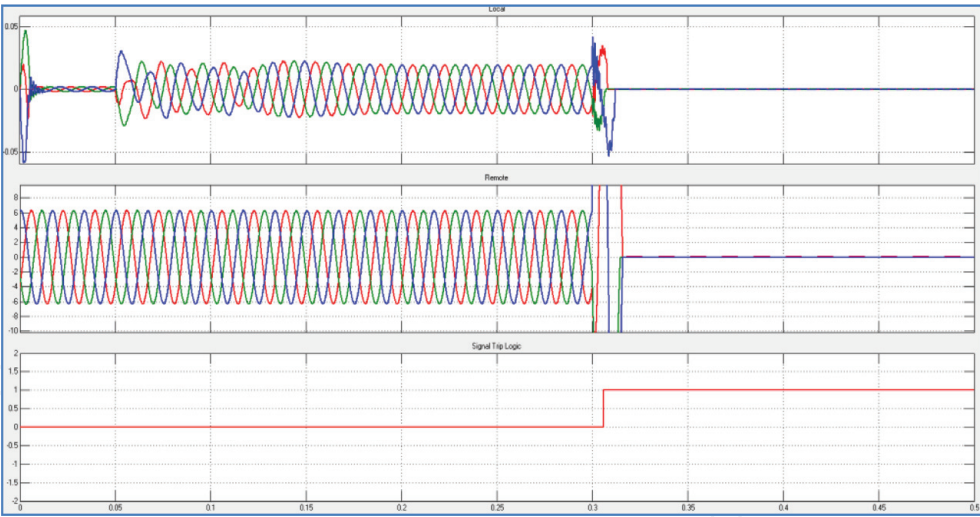


**Figure 22.**  
*3LGF current waveform.*

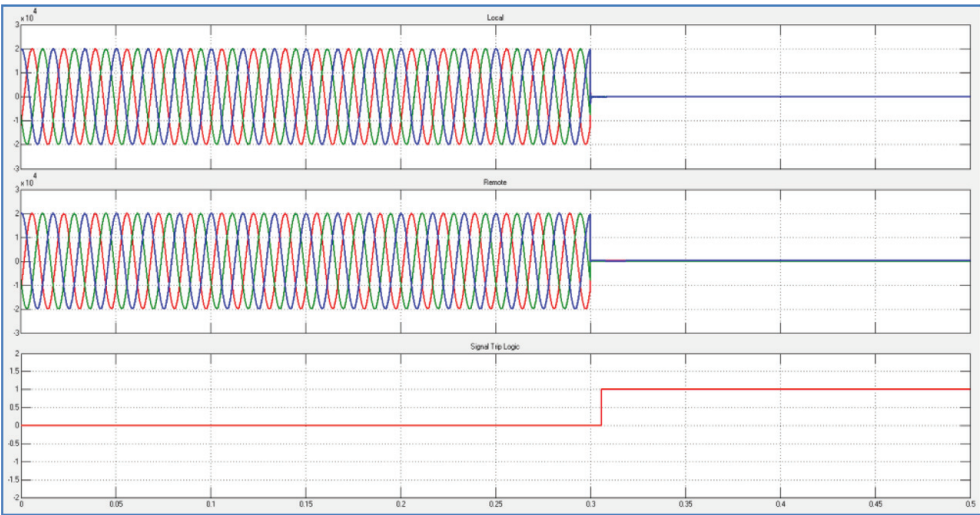


**Figure 23.**  
*3LGF voltage waveform.*

phase, namely, red, green, and blue for phases A, B, and C, respectively. The signal to Trip is represented as a binary (0, 1) measurement depending on the difference between the signals of the two ends for sending the signal to the circuit breaker. In **Figures 10–23**, two types of status are shown: for current differential and the voltage differential, with the fault occurring at  $t = 0.3$  ms.

### 7.1 Simulation result outside the protected zone

**Figures 10 and 11** show the results of an external L-G fault on protection scheme. That is differential relays without sending tripping signal.

Similarly, the results of external fault on the protection scheme in various fault conditions, that is, that mean the relay No sending trip signal to the circuit breaker.

### 7.2 Simulation result within the protected zone

**Figures 14–23** show the results of an internal fault for the protected zone. The relay sends a trip signal to the circuit breaker under a faulty condition, and the circuit breaker isolates the zone relay from the rest of the protection scheme.



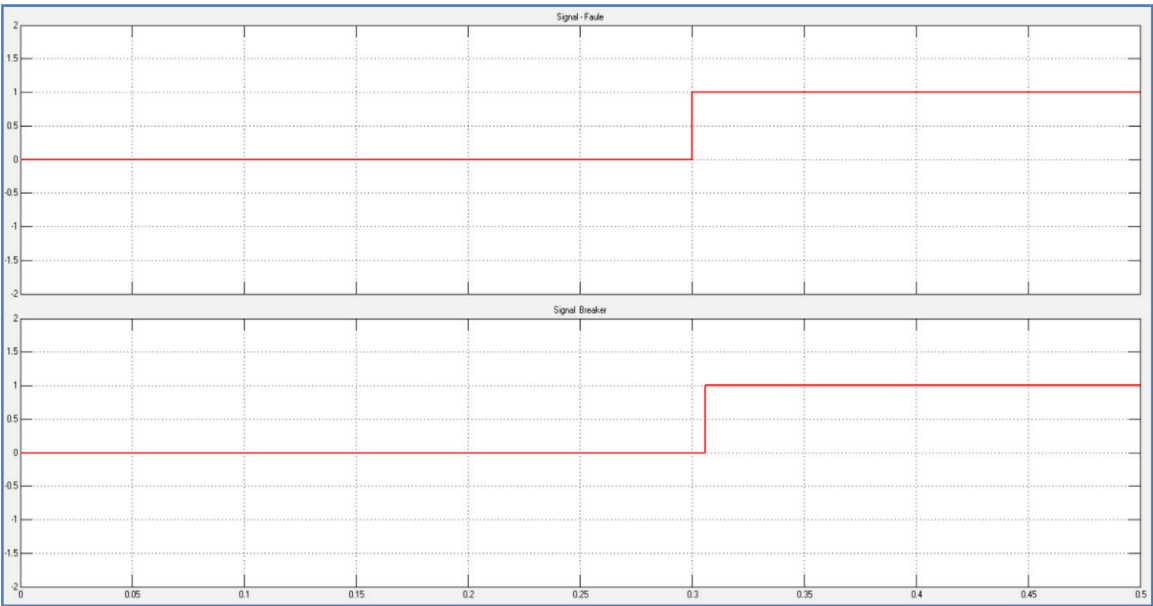


**Figure 24.**  
*The difference between the occurrence of a fault and a breaker signal.*

Measurements	Zone relay
Relay output	Trip or no trip
The threshold of operation	$t = 0.3 \text{ ms}$
Decision speed	Less than one cycle

**Table 3.**  
*Specifications of the proposed relay.*

**Figure 24** shows the time differences between the moment of a fault and signal of the breaker during and after the occurrence of the fault (**Table 3**). Displays the output of our proposed relay measurements; compared with the traditional behaviour in normal operation, the speed of our proposed scheme is less than one cycle.

## 8. Summary

The reliability of the relay protection system can be described in two respects: dependability and security. The reliability of the relay protection system detects and disconnects all faults in the protection zone. The safety of the relay protection system is capable of rejecting all events and transients that are not faulty so that the healthy part of the power system is not unnecessarily disconnected. Differential protection is the preferred solution for widespread use; fault protection for multi-terminal systems becomes very difficult, and fast fault detection of systems becomes very important. This result provides different solutions for transmission line protection. This method is better than distance protection because differential protection requires fewer input data and reduces computation time.

The performance of this algorithm is more efficient than distance relay protection. The disadvantages of the distance on the transmission line and the directional over-current relay are as follows:

1. If a fault occurs at the end of the line, the relay cannot be disconnected immediately at both ends of the line.

2. Coordination is achieved by adjusting the time delay of the relays installed on the power line beside the primary protection and backup protection. Therefore, the delay time of the relay operating in each protection zone will slow down the termination of the interference.

The differential protection principle is based on Kirchhoff current law, which has been widely used in the primary equipment protection of the power systems. The general objective of the protection system is to quickly isolate the areas that contain unrest while preserving the rest of the system. The method of protection must meet five criteria to perform successfully: (1) reliability, (2) selectivity, (3) speed, (4) simplicity, and (5) economy.

## Acknowledgements

The author would like to thank the editor and reviewers for their constructive comments and suggestions on this article. This work was supported by the Southern Technical University-Iraq, BETC, and the Huazhong University of Science and Technology-China (no. 01122018).

## Conflicts of interest

The authors declare no conflicts of interest.

## Author contributions

I would like to express my deep appreciation to Ms. Janan Abd Ali al-Hajji, also to Dr. Shaorong Wang (HUST), who oversaw my studies, and to the editor of books IntechOpen Dr. Ahmed Zobaa and Dr. Alfredo Vaccaro, I have the honor of working with them and join them.

## Author details


Ali Hadi Abdulwahid<sup>1,2\*</sup> and Adnan A. Ateeq<sup>2</sup>

1 School of Electrical and Electronic Engineering, Huazhong University of Science and Technology, Wuhan, Hubei, China

2 Department of Engineering Electrical Power, Engineering Technical College, Southern Technical University, Basra, Iraq

\*Address all correspondence to: dr.alhajji\_ali@yahoo.com

## IntechOpen

© 2019 The Author(s). Licensee IntechOpen. This chapter is distributed under the terms of the Creative Commons Attribution License (<http://creativecommons.org/licenses/by/3.0>), which permits unrestricted use, distribution, and reproduction in any medium, provided the original work is properly cited. 



## References

- [1] Ahmad A, Hassan NU. Smart Grid as a Solution for Renewable and Efficient Energy. 2016
- [2] Tong C, Wang Q, Gao Y, Tong M, Luo J. Dynamic lightning protection of smart grid distribution system. *Electric Power Systems Research*. 2014;**113**: 228-236
- [3] Muhammad Ramadan BMS, Chiang Jia Hao E, Logenthiran T, Naayagi RT, Woo WL. Islanding detection of distributed generator in presence of fault events. In: *Proceedings of the IEEE Region 10 Conference (TENCON)*; 5-8 November 2017
- [4] Muhammad Ramadan BMS, Surian R, Logenthiran T, Naayagi RT, Woo WL. Self-healing Network Instigated by Distributed Energy
- [5] Muhammad Ramadan BMS, Logenthiran T, Naayagi RT, Su C. Accelerated lambda iteration method for solving economic dispatch with transmission line losses management. In: *Proceedings of IEEE PES Innovative Smart Grid Technologies (ISGT Asia) Conference*; 2016. pp. 138-143
- [6] Logenthiran T, Naayagi RT, Woo WL, Phan V-T, Abidi K. Intelligent control system for microgrids using multi-agent system. *IEEE Journal of Emerging and Selected Topics in Power Electronics*. 2015;**3**(4):1036-1045
- [7] Zhang J, Dong Y. Power-aware communication management for reliable remote relay protection in smart grid. In: *IEEE Power Systems Conference*; 2016. pp. 1-6
- [8] Artale G, Cataliotti A, Cosentino V, Di D, Nguyen N, Russotto P, et al. Hybrid passive and communications-based methods for islanding detection in medium and low voltage smart grids. In: *Proceedings of International Conference on Power Engineering Energy and Electrical Drives Powereng-2013*; May 2013. pp. 1563-1567
- [9] Artale G, Cataliotti A, Cosentino V, Di D, Nguyen N, Tinè G. Measurement and communication interfaces for distributed generation in smart grids. In: *Proceedings of 2013 IEEE International Workshop on Applied Measurements for Power Systems AMPS*; 2013. 2013. pp. 103-107
- [10] Safdar S, Hamdaoui B, Cotilla-Sanchez E, Guizani M. A survey on communication infrastructure for micro-grids. In: *Wireless Communications and Mobile Computing Conference (IWCMC) 2013 9th International*; July 2013. pp. 1-5
- [11] Pengcheng Z. IEC 61850-9-2 process bus communication Interface for light weight merging unit testing environment: Thesis. Stockholm, Sweden: KTH Electrical Engineering; 2012
- [12] Wibowo H, Ary PN, Hidayat S. Design and testing of Rogowski coil based PCB double helix for gas insulated switchgear 150 kV application. In: *Power Engineering and Renewable Energy (ICPERE)*; 2016 3rd Conference on. IEEE. 2017
- [13] Elkalashy NI, Kawady TA, Esmail EM, Taalab AI. Fundamental current phasor tracking using DFT extraction of Rogowski coil signal. *IET Science, Measurement and Technology*. 2016; **10**(4):296-305
- [14] Hajipour E, Vakilian M, Pasand MS. Current-transformer saturation compensation for transformer differential relays. *IEEE Transactions on Power Delivery*. 2015;**30**(5):2293-2302
- [15] Metwally IA. Novel designs of wideband Rogowski coils for high

- pulsed current measurement. IET Science, Measurement and Technology. 2014;8(1):9-16
- [16] Hemmati E, Shahrtash SM. Digital compensation of Rogowski coil's output voltage. IEEE Transactions on Instrumentation and Measurement. 2013;62(1):71-82
- [17] Al-Sowayan S. Improved mutual inductance of Rogowski coil using hexagonal core. International Journal of Electrical and Computer Engineering Electronic and Communication Engineering. 2014;8(2):293-296
- [18] Marracci M, Tellini B. Analysis of precision Rogowski coil via analytical method and effective cross section parameter. In: Proc. IEEE I2MTC; 23–26 May 2016; 2016. pp. 1-5
- [19] Vourc'h E, Yu W, Joubert P-Y, Revol B, Couderette A, Cima L. Neel effect toroidal current sensor. IEEE Transactions on Magnetics. 2013;49(1): 81-84
- [20] Raspolli AM, Antonetti C, Marracci M, Piccinelli F, Tellini B. Novel microwave-synthesis of Cu nanoparticles in the absence of any stabilizing agent and their antibacterial and antistatic applications. Applied Surface Science. 2013;280:610-618
- [21] Ramesh K, Sushama M. Power transformer protection using fuzzy logic based-relaying. In: International Conference on Advances in Electrical Engineering; 2014. pp. 1-7
- [22] Deshmukh MS, Barhate VT. Transformer protection by distinguishing inrush and fault current with harmonic analysis using fuzzy logic. In: IEEE International Conference on Control and Robotics Engineering; April 2016
- [23] Barhate V, Thakre KL, Deshmukh M. Adaptable differential relay using fuzzy logic code in digital signal controller for transformer. In: 57th International Scientific Conference on Power and Electrical Engineering of Riga Technical University (RTUCON); October 2016
- [24] Paz MCR, Leborgne RC, Bretas AS. Adaptive ground distance protection for UPFC compensated transmission lines: A formulation considering the fault resistance effect. International Journal of Electrical Power & Energy Systems. 2015;73:124-131
- [25] Han KL, Cai ZX, Xu M, Hi Z. He dynamic characteristics of characteristic parameters of traveling wave protection for HVDC transmission line and their setting. Power System technology. 2013; 37:255-260
- [26] Tavares KA, Silva KM. Modeling and simulation of the differential protection of power transformers in EMTP Softwares. In: DPSP: International Conference on Developments in Power System Protection; 2012
- [27] Alvarenga MTS, Vianna PL, Silva KM. High-impedance bus differential protection modeling in ATP/MODELS. Engineering. 2013;5:37-42
- [28] Franklin R, Nabi-Bidhendi H, Thompson MJ, Altuve HJ. High-impedance differential applications with mismatched CTs. In: Proceedings of the 44th Annual Western Protective Relay Conference; October 2017